

Quantal Phases in Polarimetry

Peter Larsson

February 28, 2003

this page intentionally left blank

Quantal Phases in Polarimetry

Peter Larsson

February 27, 2003

Abstract

The first part of this thesis presents a theoretical and experimental background to the subject of quantal phases. Some of the topics covered are: Pancharatnam's phase, parallel transport, the quantum kinematic approach to geometric phases, mixed state (geometric) phases, and the polarimetric and interferometric ways of measuring phases experimentally. The second part deals with quantal phases in polarimetry and demonstrates how to measure phases for pure systems with spin $> \frac{1}{2}$ and for mixed spin- $\frac{1}{2}$ systems by polarimetry. It is shown that the polarimetric method proposed by Wagh and Rakhecha [Phys. Lett. A 197:112-115] for measuring the phase of spin- $\frac{1}{2}$ particles can be used for more complex systems as well, albeit with some modifications and considerably more involved analysis for extracting the phase.

this page intentionally left blank

Contents

1	Phase fundamentals	5
1.1	Pancharatnam's phase	6
1.2	Parallel transport	8
1.3	Quantum kinematic approach	9
1.4	Berry's original phase	12
1.5	The geometric phase of Aharonov and Anandan	13
2	Mixed state phases	15
2.1	Uhlmann's phase	16
2.2	Sjöqvist <i>et al.</i> 's phase	17
2.3	Comparison of mixed state geometric phases	20
3	Experimental phase measurements	21
3.1	Strategies for observing phases	22
3.2	Polarimetric setup	23
3.3	Interferometric setup	25
3.4	Polarimetry vs. Interferometry	26
4	Measuring higher-spin phases	27
4.1	SO(3) polarimetry on higher spin states	27
4.2	The $ j \pm j\rangle$ case	28
4.3	The general $ jm\rangle$ case	30
5	Mixed states in polarimetry	35
5.1	Evolution of the mixed state	35
5.2	Generalizing the pure state Pancharatnam phase to the mixed state .	36
5.3	Reverse engineering the mixed state phase found in interferometry	37
5.4	Measuring the degree of mixing	38

this page intentionally left blank

Preface

This text comprises my thesis for the degree of Master of Science in Physics at Uppsala University. The subject is quantum mechanics. Although the mathematics have turned out to be exceptionally easy, the reader is still assumed to possess knowledge of quantum mechanics at an intermediate level (i.e. ray spaces and some group theoretical aspects of quantum mechanics). The larger part of the text describes the theoretical and experimental background of the subject. It should be sufficient to allow the reader to follow the ideas developed later, but can in no way replace the original literature. My intent has rather been to present ideas and concepts that are not always easily extracted from the original papers. In that way, the background text represent an introduction that I would like to have had myself when going through existing papers. A few principles have guided the text:

- **Simplicity:** sometimes by sacrificing a bit of clarity. It is my belief that a horribly looking formula may not be read at all, no matter how precise the notation is. To ease the burden, I have tried to omit indices, use standard symbols, and keep expressions to a single line, when possible. $\hbar = 1$.
- **Completeness:** derivations connected to new claims have been presented with many, sometimes, simple steps, while calculations related to examples and reformulations have not.
- **Readability:** not too long lines and paragraphs; text set in 12pt.

Happy reading!

Peter Larsson
February 2003

this page intentionally left blank

Prologue

This thesis deals with quantum mechanics. During my time working with quantum mechanics, I have come to view it as a labyrinth; a large building the student learns to enter by any of a number of doors. Once established in my mind, it came to have the feel of an implant, something useful, but still alien. It thrives there, however, on my mind's horizon, exerting its own peculiar attraction; slowly sending out its entangling roots. It is a singularity of classical physics.

My own doors to quantum mechanics were chemistry and mathematics. Sometimes it helped, sometimes it did not. Being raised in the atomic world, far from Newtonian mechanics, the effects of quantum mechanics were never as peculiar to me, I think, as for the classical physicist. On the other hand, it can hardly be denied that much of the structure of quantum mechanics is far more accessible from a classical angle of attack.

Exploring quantum mechanics has been like walking down a hall, opening doors. You open a door on your left, and something very nasty jumps out at you. You open a door on your right, and you find the solution to your problems piled up elegantly in a corner. I cannot say that I have understood it. Sometimes, I feel that I have almost understood it, or that I was coming close to understanding it. Strangely enough, this has never caused me any discomfort, or prevented me from taking pleasure in the subject. On the contrary, the opposite has been true; trusting logic in lands where intuition fails has been most rewarding. In fact, I would argue, quantum mechanics is not meant to be understood in the first place.

As an example, when I first ventured into this area of quantum mechanics I discovered that I had this naive, realistic view about operators. Somewhere, probably from the basic courses in quantum mechanics, I had picked up, and believed, a bit too strongly in the idea of the operator as an observable. Quantal phases are perhaps the prime example of a violation of this idea. They are observable properties of a quantum system that are, at least not presently, known to correspond to any self-adjoint operators. In that perspective, they represent some of the oddballs I have found, stumbling through the labyrinth.

this page intentionally left blank

Chapter 1

Phase fundamentals

When a quantum system undergoes a cyclic evolution, the initial and final wave functions can differ by at most a phase factor, since the initial state should be the same as the final state. No measurement can determine the phase of a single wave function: the two states $|\psi\rangle$ and $e^{i\phi}|\psi\rangle$ are indistinguishable.

What can be determined, however, is the phase difference between states. In 1984, interest in phases arose when Berry [1] published a very influential paper concerning the existence of a *geometric phase* in association with cyclic adiabatic evolution. The term "geometric phase" is a component of the total phase that depends only on the sequence of states that the system has been in, and not on the exact dynamics of how these states have been visited during the evolution. This new phase of geometric origin turned out to have many surprising properties such as: being observable, despite the fact that it cannot be expressed as an expectation value; being not at all dependent on adiabatic or cyclic evolution [2, 3]; and being able to provide insights into several mysterious phenomena such as the Aharonov-Bohm effect.

Most presentations concerning geometric phases typically start by first describing Berry's discovery and then progressively move on to more general treatments and advanced concepts. I intend to do the opposite because I believe that there is a significant pedagogical advantage in first describing the general case and then working out the details. Therefore, we will start by looking at Pancharatnam's original triangle phase and Bargmann invariants and quite quickly arrive at the very essence of the geometric phase. Then we will investigate the quantum kinematic approach by Mukunda and Simon. Finally, the special case of Berry's cyclic adiabatic evolution will be considered and related to the described framework. Armed with this knowledge of pure state phases the concept of phases for mixed states will be introduced in the next chapter.

1.1 Pancharatnam's phase

The geometric phase was discovered as early as 1956 by the Indian physicist Pancharatnam [4] while he was studying optical interference between light beams. Unfortunately, his anticipation of the geometric phase did not receive adequate attention at that time and was forgotten for almost 40 years. It was not until after Berry's paper that the significance of Pancharatnam's work was identified [5, 6].

We will look at Pancharatnam's phase from a polarimetric perspective. Imagine two different mutually non-orthogonal state vectors $|\Psi_0\rangle$ and $|\Psi_1\rangle$ in a Hilbert space. If a system evolves from $|\Psi_0\rangle$ to $|\Psi_1\rangle$ in a completely general way, one may ask if it possible to find a relative phase between the two state vectors. In his paper Pancharatnam assigned such a relative phase Φ between the two states using the expression:

$$\Phi = \arg\langle\Psi_0|\Psi_1\rangle. \quad (1.1)$$

Although the usual rationale for this phase difference is based on introducing a variable phase shift to one of the state vectors and looking at the maximal interference with the other state vector, it can also be derived by the following simple reasoning. Let us attempt to get a phase difference between $|\Psi_0\rangle$ and $|\Psi_1\rangle$ by projecting $|\Psi_1\rangle$ onto $|\Psi_0\rangle$ and normalize the result:

$$|\Psi_0\rangle' = \frac{|\Psi_0\rangle\langle\Psi_0|\Psi_1\rangle}{|\langle\Psi_0|\Psi_1\rangle|}. \quad (1.2)$$

Now $|\Psi_0\rangle'$ and $|\Psi_0\rangle$ represent the same state. Consequently they differ by at most a phase factor. We take this phase to be our relative phase Φ and evaluate it as:

$$\begin{aligned} e^{i\Phi} &\equiv \langle\Psi_0|\Psi_0\rangle' = \frac{\langle\Psi_0|\Psi_1\rangle}{|\langle\Psi_0|\Psi_1\rangle|} \Rightarrow \\ \Phi &= \arg\langle\Psi_0|\Psi_1\rangle. \end{aligned} \quad (1.3)$$

Pancharatnam's relative phase is what we will call the *total* phase, containing all phase contributions that the system acquires during its evolution. From basic quantum mechanics we know that one such phase is the *dynamical* phase resulting from interaction with the environment described by the Hamiltonian. But does it contain anything else?

Looking for an answer, we now turn to Pancharatnam's optical experiment. It consists of polarized light passing through a series of polarizers which successively filters out light with a particular polarization direction (fig. 1.1). Using quantum mechanics, each polarization state can be represented by a quantum state of the photon. Let us call these photon states Ψ_0 , Ψ_1 and Ψ_2 . What is Pancharatnam's relative phase between $|\Psi_0\rangle$ and $|\Psi_2\rangle$? From fig. 1 we see that:

$$|\Psi_2\rangle' = \frac{|\Psi_2\rangle\langle\Psi_2|\Psi_1\rangle\langle\Psi_1|\Psi_0\rangle}{|\langle\Psi_2|\Psi_1\rangle\langle\Psi_1|\Psi_0\rangle|} \Rightarrow \quad (1.4)$$

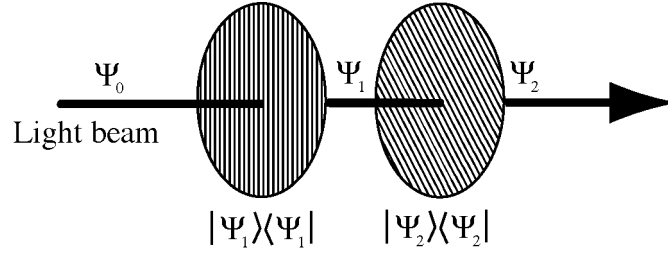


Figure 1.1: The optical set-up used by Pancharatnam.

$$\Phi = \arg\langle\Psi_0|\Psi_2\rangle' = \arg\langle\Psi_0|\Psi_2\rangle\langle\Psi_2|\Psi_1\rangle\langle\Psi_1|\Psi_0\rangle. \quad (1.5)$$

It is now clear that all the dynamical phases cancel in pairs, making the phase (1.5) independent of the particular Hamiltonian. It does, however, depend on which states the system evolves into and the sequence of these states. This dynamical phase independent quantity is what makes up the *geometric* phase. If we look at how the evolution of the polarization state looks like in the ray space (fig. 1.2) it is easy to see why this phase is called "geometric". It can be shown that the solid angle enclosed by the sequence of polarization states on the Poincaré sphere corresponds directly to the phase, thus giving it a geometric interpretation. Expressions of the type described by (1.5) are sometimes called "Bargmann invariants" after a paper by Bargmann [7] in 1964, where he used them in a different context to prove Wigner's theorem.

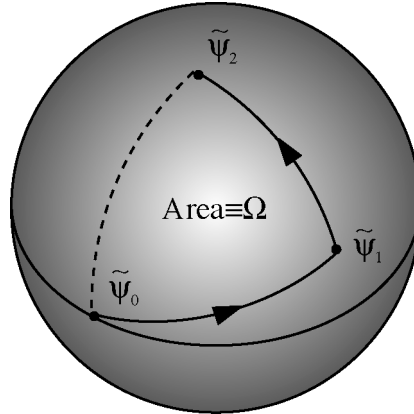


Figure 1.2: Pancharatnam triangle in the polarization ray space. The ray space for a two-level system can be pictured as the surface of a sphere. Two successive filtering measurements move the system to different states (points) along geodesics. Despite the fact that filtering is phase-preserving, the procedure yields a geometric phase of $-\Omega/2$.

1.2 Parallel transport

At first, one might think that the peculiar effects of the geometric phase are limited to quantum mechanics. We shall see, however, that the geometric phase can be realized in classical systems as well [8], using the concept of parallel transport of vectors.

When a vector is moved along a path on a surface, the vector is said to undergo parallel transportation if it is not rotated around the normal vector of the surface at any time. If the path is closed so that the vector returns to its original position, our intuition tells us that the initial and the final vectors should be parallel. On a flat surface, this is certainly the case but on a curved surface it is not so. The most famous example is the parallel transportation of a vector on a sphere (fig. 1.3).

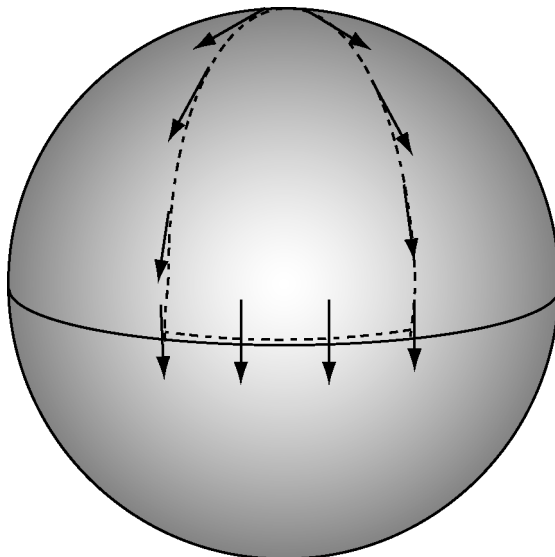


Figure 1.3: Parallel transport on a two-dimensional sphere. A vector starts at the north pole and moves along the dashed line. When it returns to the north pole it has acquired a rotation, which only depends on the path it followed.

From the picture it is obvious that rotations can occur although a vector quantity is parallel transported on a curved surface such as a sphere. If the curve traced by the vector is closed, the operation on the vector is called a *holonomy transformation* and the acquired rotation the *holonomy*. Remembering the spherical surface representation of the two-state ray space in figure 1.2 we see that the geometric phase is actually a manifestation of the holonomy that arises from the movement of the state on the ray space surface. The quantity being parallel transported in this case is the phase (since phases are complex numbers, which can be seen as vectors in two dimensions). This important observation will be

investigated further in the next section when we look at the quantum kinematic approach.

Another important observation from the example of parallel transport on the sphere (fig. 1.3) is that there are some paths of movement that do not give rise to a rotation. As long as the vector is transported along a geodesic, e.g. the equator, no additional rotation is acquired. This implies that there should also be some paths in the ray space that give no geometric phase, a fact that is also exploited in the next section.

1.3 Quantum kinematic approach

The quantum kinematic approach by Mukunda and Simon [9] provides a clear and thorough framework for dealing with geometric phases at the very fundamental level of quantum mechanics. Among other things, it is shown how Berry-type phases can be connected to Bargmann-like expressions by a limiting process.

Mukunda and Simon define the geometric phase associated with the evolution in Hilbert spaces. The evolution is represented by a continuous one-dimensional set of vectors $|\psi(s)\rangle$ parameterized by s . Such a set of vectors will project on a smooth curve C in the corresponding ray space. The geometric phase associated with this curve is then defined as

$$\begin{aligned} \phi_g(C) &= \arg\langle\psi(s_1)|\psi(s_2)\rangle - \text{Im} \int_{s_1}^{s_2} \langle\psi(s)|\dot{\psi}(s)\rangle ds, \\ \text{geometric phase} &= \text{total phase} - \text{dynamical phase}. \end{aligned} \quad (1.6)$$

As mentioned earlier, it is reasonable to expect that there could exist curves in ray space along which a vector does not accumulate phase changes. One of the key results of [9] is the proof of this assumption. It is shown that in every ray space there exists "geodesic" curves along which no geometric phase of the type (1.6) arises. In the next step this conclusion is supplemented by another important result: two vector projections in a ray space can always be connected by a geodesic. Together, these two notions provide the tools necessary for arriving at several interesting results.

Following Mukunda and Simon [9] we now consider an open, segmented curve (\tilde{C}) made up of $N - 1$ curve segments \tilde{G}_i in the Hilbert space (fig. 1.4). Each segment connects two state vectors with a curve that projects onto a geodesic in the ray space. For the full curve in ray space (C) we know from (1.6) that the geometric phase is

$$\phi_g(C) = \phi_{total}(\tilde{C}) - \phi_{dyn}(\tilde{C}) \quad (1.7)$$

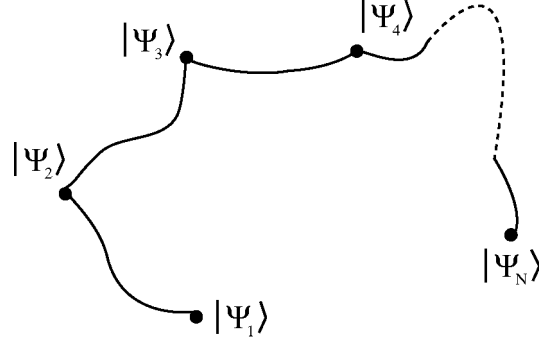


Figure 1.4: A chain of geodesics in Hilbert space connecting N state vectors.

or more explicitly

$$\phi_g(C) = \arg\langle\psi_1|\psi_N\rangle - \sum_{r=1}^{N-1} \phi_{dyn}(\tilde{G}_r). \quad (1.8)$$

Applying (1.7) again gives

$$\begin{aligned} \phi_g(C) &= \arg\langle\psi_1|\psi_N\rangle - \sum_{r=1}^{N-1} \{\phi_{total}(\tilde{G}_r) - \phi_g(\tilde{G}_r)\} \\ &= \arg\langle\psi_1|\psi_N\rangle - \sum_{r=1}^{N-1} \arg\langle\psi_r|\psi_{r+1}\rangle \\ &= -\arg\langle\psi_1|\psi_2\rangle\langle\psi_2|\psi_3\rangle\langle\psi_3|\psi_4\rangle\cdots\langle\psi_{N-1}|\psi_N\rangle\langle\psi_N|\psi_1\rangle \end{aligned} \quad (1.9)$$

due to the fact that $\phi_g(\tilde{G}_r) = 0$. We have now obtained a Bargmann-expression very much like the one from the Pancharatnam setup (1.5). We also note that cyclic permutation of the sequence of the states do not affect $\phi_g(C)$ as given by (1.9). The last factor looks like an additional contribution to the phase corresponding to a closure of the path. How does this come? Guided by this question, we calculate the geometric phase of a *closed* curve \tilde{O} in Hilbert space made up of N geodesics. Now the total phase is zero so:

$$\begin{aligned} \phi_g(O) &= \phi_{total}(\tilde{O}) - \phi_{dyn}(\tilde{O}) = -\phi_{dyn}(\tilde{O}) \\ &= -\sum_{r=1}^N \phi_{dyn}(\tilde{G}_r) \\ &= \sum_{r=1}^N \{\phi_g(\tilde{G}_r) - \phi_{total}(\tilde{G}_r)\} \\ &= -\sum_{r=1}^N \arg\langle\psi_r|\psi_{r+1}\rangle \end{aligned}$$

$$\begin{aligned}
&= -\arg\langle\psi_1|\psi_2\rangle\langle\psi_2|\psi_3\rangle\langle\psi_3|\psi_4\rangle\dots\langle\psi_{N-1}|\psi_N\rangle\langle\psi_N|\psi_1\rangle \\
&= \phi_g(C).
\end{aligned} \tag{1.10}$$

So the open curve \tilde{C} and the closed curve \tilde{O} have the same geometric phase! Closing C with a geodesic to obtain O does not add any geometric phase. This was implicitly given already in figure 1.2, where the area would have been the same even if the curve was completed, and may not come as a surprise. Here, however, we have proved it for general Hilbert spaces and showed that there is no essential difference between cyclic and noncyclic evolutions. Geometric phases for noncyclic evolutions can be calculated by completing the evolution to a cyclic one with a geodesic curve and evaluating the resulting cyclic phase. Or conversely, geometric phases can be analyzed for open paths without losing generality.

Finally, we look at how the geometric phase for a smooth curve (1.6) can be obtained from Bargmann-like expressions. The idea in [9] is to approximate the smooth curve by an increasing number of short geodesics (fig. 5).

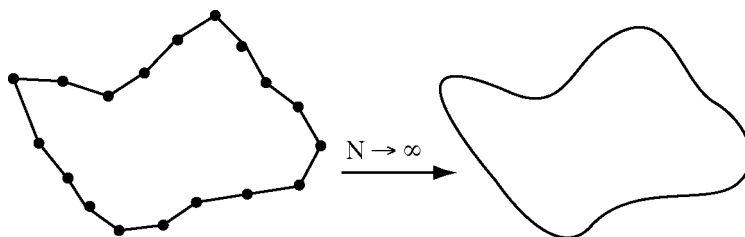


Figure 1.5: Approximating a smooth curve with a chain of geodesics. When the number of geodesics becomes infinite, the curve becomes smooth.

If we start with a curve made up of N geodesics connecting $N + 1$ states, such as in (1.10), we have

$$\phi_g(C) = -\arg\langle\psi_1|\psi_2\rangle\langle\psi_2|\psi_3\rangle\langle\psi_3|\psi_4\rangle\dots\langle\psi_N|\psi_{N+1}\rangle\langle\psi_{N+1}|\psi_1\rangle. \tag{1.11}$$

Letting $N \rightarrow \infty$ and introducing a parameter range $s_1 \leq s \leq s_2$ gives

$$\phi_g(C) = \lim_{N \rightarrow \infty} \left\{ \arg\langle\psi(s_1)|\psi(s_2)\rangle - \arg \prod_{n=1}^N \langle\psi(\sigma_n)|\psi(\sigma_{n+1})\rangle \right\} \tag{1.12}$$

where the parameters σ_n specify ψ so that $\psi(\sigma_n) = \psi_n$. A number of approximations then produce the geometric phase for the smooth curve:

$$\begin{aligned}
\phi_g(C) &\approx \lim_{N \rightarrow \infty} \left\{ \arg\langle\psi(s_1)|\psi(s_2)\rangle - \arg \prod_{n=1}^N \langle\psi(\sigma_n)|\psi(\sigma_n) + \Delta s \dot{\psi}(\sigma_n)\rangle \right\} \\
&= \lim_{N \rightarrow \infty} \left\{ \arg\langle\psi(s_1)|\psi(s_2)\rangle - \arg \prod_{n=1}^N [1 + \Delta s \langle\psi(\sigma_n)|\dot{\psi}(\sigma_n)\rangle] \right\}
\end{aligned}$$

$$\begin{aligned}
&\approx \lim_{N \rightarrow \infty} \left\{ \arg \langle \psi(s_1) | \psi(s_2) \rangle - \arg \exp \left(\sum_{n=1}^N \langle \psi(\sigma_n) | \dot{\psi}(\sigma_n) \rangle \Delta s \right) \right\} \\
&= \arg \langle \psi(s_1) | \psi(s_2) \rangle - \arg \exp \left(i \operatorname{Im} \int_{s_1}^{s_2} \langle \psi(s) | \dot{\psi}(s) \rangle ds \right) \\
&= \arg \langle \psi(s_1) | \psi(s_2) \rangle - \operatorname{Im} \int_{s_1}^{s_2} \langle \psi(s) | \dot{\psi}(s) \rangle ds. \tag{1.13}
\end{aligned}$$

Thus we have seen how Bargmann-like expressions are connected to the geometric phases associated with discrete as well as smooth evolutions. Everything has been based on strictly kinematic concepts in ray space, without relating to a specific Hamiltonian. Thus, geometric phases stem solely from the geometry of the ray space, which explains the general applicability of the quantum kinematic approach. As an example, we will look at the geometric phase found by Berry [1] within our new framework in the next section.

1.4 Berry's original phase

According to the adiabatic theorem, a system governed by a changing Hamiltonian will always be in an eigenstate to the instantaneous Hamiltonian, provided that the Hamiltonian is only slowly altered and the system is initially put in an eigenstate. When the evolution is cyclic so that Hamiltonian returns to its original form, the system will also return to its original state, but multiplied by a phase factor. Berry discovered that in addition to the expected dynamical phase factor, there is an additional phase factor, which is independent of the Hamiltonian. Using (1.13) we will now see that Berry's phase factor is the same as that corresponding to the geometric phase we studied earlier.

When using the approximation provided by the adiabatic theorem a solution to the time-dependent Schrödinger equation is [9]

$$|\psi(t)\rangle = \exp \left(i\gamma(t) - i \int_0^t E(t') dt' \right) |\phi(t)\rangle, \tag{1.14}$$

where $|\phi(t)\rangle$ is the instantaneous eigenvector of the Hamiltonian at time t and $\gamma(t)$ is Berry's phase factor. We assume that $\gamma(0) = 0$. If the evolution is cyclic and returns to the initial state at time T , the final state is

$$|\psi(T)\rangle = \exp \left(i\gamma(T) - i \int_0^T E(t) dt \right) |\psi(0)\rangle. \tag{1.15}$$

This solution will trace out a closed curve in the ray space since $\tilde{\psi}(T) = \tilde{\psi}(0)$. Based on the results mention earlier (1.6,1.13) we know how to calculated the

geometric phase for such a curve. We find:

$$\phi_{total} = \arg\langle\psi(0)|\psi(T)\rangle = \gamma(T) - \int_0^T E(t) dt, \quad (1.16)$$

$$\begin{aligned} \phi_{dyn} &= \text{Im} \int_0^T \langle\psi(t)|\dot{\psi}(t)\rangle dt \\ &= - \int_0^T \langle\psi(t)|H(t)|\psi(t)\rangle dt \approx - \int_0^T E(t) dt, \end{aligned} \quad (1.17)$$

$$\phi_g = \phi_{total} - \phi_{dyn} = \gamma(T). \quad (1.18)$$

Inserting (1.18) into (1.15) shows very clearly the nature of the phase factor discovered by Berry:

$$|\psi(t)\rangle = \exp\left(i\phi_g - i \int_0^t E(t') dt'\right) |\phi(t)\rangle. \quad (1.19)$$

The extra phase factor γ , which was thrown in as a placeholder, turns out to be a geometric phase, dependent only upon the path of the system in the ray space. In Berry's paper, however, the geometric nature was not attributed to the ray space, but rather to the space of the parameters $\mathbf{R}(t)$ that control the Hamiltonian. The curve traced in the parameter space by the system was shown to solely determine the geometric phase. This apparent discrepancy is explained by the adiabatic condition: it makes the geometry of the parameter space coincide exactly with that in the ray space, thus enabling Berry to study the underlying ray space properties in the parameter space.

1.5 The geometric phase of Aharonov and Anandan

The geometric phase discovered by Berry was soon generalized to nonadiabatic cyclic evolutions by Aharonov and Anandan [2]. This was partly motivated by the fact that the Aharonov-Bohm phase could be derived from Berry's phase expression, even though the former is independent of the adiabatic condition.

With no adiabatic condition we are left with just the following assumption:

$$|\psi(T)\rangle = e^{i\varphi} |\psi(0)\rangle. \quad (1.20)$$

Such an evolution will trace out a closed curve in ray space, so the geometric phase can be evaluated from (1.6) as:

$$\begin{aligned} \phi_{total} &= \arg\langle\psi(0)|\psi(T)\rangle = \varphi \\ \phi_{dyn.} &= \text{Im} \int_0^T \langle\psi(t)|\dot{\psi}(t)\rangle dt = - \int_0^T \langle\psi(t)|H(t)|\psi(t)\rangle dt \\ \phi_g &= \varphi + \int_0^T \langle\psi(t)|H(t)|\psi(t)\rangle dt. \end{aligned} \quad (1.21)$$

Inserting (1.21) into (1.20) shows that the geometric part of the phase is still present in the nonadiabatic case:

$$|\psi(T)\rangle = \exp\left(i\phi_g - i \int_0^T \langle \psi(t) | H(t) | \psi(t) \rangle dt\right) |\psi(0)\rangle, \quad (1.22)$$

which is one of the two important results in the work of Aharonov and Anandan. The other important result was that their new geometric phase is completely determined by the curve in ray space. This fact is already built-in in our quantum kinematic approach, however, so we will not investigate it further here.

Chapter 2

Mixed state phases

The previous chapter dealt with phases within the pure state formalism of quantum mechanics. In many cases it is necessary to consider statistical ensembles of quantum systems, for example, when we are interested in measuring probability distributions. Other situations include NMR experiments and modelling of decoherence. Statistical ensembles containing many pure states are represented by density operators:

$$\rho = \sum_{i=0}^{N-1} w_i |i\rangle\langle i| \quad (2.1)$$

and called *mixed states*. If ρ cannot be expressed as a single projection operator $|\psi\rangle\langle\psi|$ it represents a *nonpure* state. N is the dimension of the Hilbert space and w_i is the fraction of systems in the state $|i\rangle$ within the ensemble. Consequently, the trace of any normalized density operator is 1.

Interest in geometrical phases for mixed states has primarily been driven by advances in the theory of quantum computing. A major problem in realizing quantum computation is protecting the system from environmental noise and decoherence. Geometric phases are thought to be more fault-tolerant in such situations, and it has been shown that quantum computing could be performed with geometric phases using NMR [10]. In such contexts mixed states enter naturally to describe the particles in the magnetic field.

There are, however, different ways to extend the concept of geometric phase to mixed states [11, 12]. Uhlmann [11] was the first to consider holonomies in the space of density operators, but presently, no way of actually measuring his phase has been found (cf. [13] for a proposed two-particle setup). The main reason is probably that Uhlmann's phase is based on mathematical, rather than physical ideas. Later, an experimental approach to mixed state phases was proposed by Sjöqvist *et al.* [12]. Their phase is derived within the context of interferometry and is possible to observe as a shift of interference oscillations.

2.1 Uhlmann's phase

A natural way to generalize the geometric phase to density operators would be to write Bargmann expressions again and replace the wave functions with density operators. Unfortunately, this is not possible because the density operators do not form a Hilbert space and cannot be manipulated in the same way as pure states.

Instead, Uhlmann's approach [11] starts by using a purification (a so-called 'GNS construction', see e.g. [14]) to get a Hilbert space from the density operators. Physically, this is equivalent to embedding the mixed state into a larger system in which it can be seen as a reduction of a pure state. The extended Hilbert space is isomorphic to the Hilbert space of the Hilbert-Schmidt operators. Conveniently, the square root of the density matrix is a Hilbert-Schmidt operator and can be used to represent the mixed state. In symbols:

$$\rho = WW^\dagger \quad \text{and} \quad W = \sqrt{\rho}U, \quad (2.2)$$

where W is a Hilbert-Schmidt operator and U an arbitrary unitary operator that Uhlmann calls the "phase factor". The inner product between two Hilbert-Schmidt operators is

$$\langle W_1, W_2 \rangle = \text{Tr}(W_1^\dagger W_2). \quad (2.3)$$

Within this framework we can now make an *ansatz*: let us assume that the geometric phase for a sequence of density operators can be calculated from Bargmann expressions as well. Analogously we would then have

$$\phi_g(\Pi) = \arg\langle W_1, W_2 \rangle \langle W_2, W_3 \rangle \dots \langle W_{N-1}, W_N \rangle \langle W_N, W_1 \rangle \quad (2.4)$$

for the ordered set $\Pi = \{W_1, W_2, \dots, W_N\}$ of Hilbert-Schmidt operators that represent our density operators. Is this reasonable? Our first concern should be to investigate whether this expression is of truly geometric nature, so that it depends only on the sequence of states described by the density operators. Uhlmann showed that this requirement is met when we choose the U -operators in (2.2) to maximize (2.4), which amounts to

$$|\langle W_n, W_{n+1} \rangle| = \text{Tr} \sqrt{\sqrt{\rho_{n+1}} \rho_n \sqrt{\rho_{n+1}}}. \quad (2.5)$$

The second concern would be if our new phase for density operators reduces to the one for pure states when $\rho = |\psi\rangle\langle\psi|$. To investigate this we evaluate the inner product in (2.3) of two pure states $\rho_1 = |\psi_1\rangle\langle\psi_1|$ and $\rho_2 = |\psi_2\rangle\langle\psi_2|$:

$$\begin{aligned} \langle W_1, W_2 \rangle &= \text{Tr}(W_1^\dagger W_2) = \text{Tr}(U_1^\dagger \sqrt{\rho_1} \sqrt{\rho_2} U_2) \\ &= \text{Tr}(U_1^\dagger \rho_1 \rho_2 U_2) = \text{Tr}(U_1^\dagger |\psi_1\rangle\langle\psi_1| \langle\psi_1|\psi_2\rangle \langle\psi_2| U_2) \\ &= \langle\psi_1|\psi_2\rangle \langle\psi_2| U_2 U_1^\dagger |\psi_1\rangle. \end{aligned} \quad (2.6)$$

Making use of the maximality constraint (2.5) we get:

$$|\langle W_1, W_2 \rangle|^2 = \text{Tr} \sqrt{\rho_1} \rho_2 \sqrt{\rho_1} = \text{Tr}(\rho_1 \rho_2 \rho_1) = |\langle \psi_1 | \psi_2 \rangle|^2. \quad (2.7)$$

But from (2.6) we also know that:

$$|\langle W_1, W_2 \rangle|^2 = |\langle \psi_1 | \psi_2 \rangle|^2 \cdot |\langle \psi_2 | U_2 U_1^\dagger | \psi_1 \rangle|^2 \quad (2.8)$$

$$\Rightarrow |\langle \psi_2 | U_2 U_1^\dagger | \psi_1 \rangle| = 1. \quad (2.9)$$

This implies that the scalar product of our two Hilbert-Schmidt operators reduces to the pure state scalar product up to an arbitrary phase factor:

$$\langle W_1, W_2 \rangle = \langle \psi_1 | \psi_2 \rangle e^{-i \arg \langle \psi_2 | U_2 U_1^\dagger | \psi_1 \rangle}. \quad (2.10)$$

When these scalar products are put together to form a Bargmann-invariant, we get the pure state invariant and an additional phase factor $e^{-i\delta}$:

$$\begin{aligned} \phi_g(\Pi) &= \arg \langle W_1, W_2 \rangle \langle W_2, W_3 \rangle \dots \langle W_{N-1}, W_N \rangle \langle W_N, W_1 \rangle \\ &= \arg \langle \psi_1 | \psi_2 \rangle \langle \psi_2 | \psi_3 \rangle \dots \langle \psi_{N-1} | \psi_N \rangle \langle \psi_N | \psi_1 \rangle e^{-i\delta}. \end{aligned} \quad (2.11)$$

But looking at δ we see that:

$$\begin{aligned} \delta &= \arg \text{Tr}(U_N^\dagger | \psi_N \rangle \langle \psi_N | U_N \dots U_1^\dagger | \psi_1 \rangle \langle \psi_1 | U_1) \\ &= \arg \text{Tr}(P_N \dots P_1) = 0. \end{aligned} \quad (2.12)$$

This makes (2.11) equivalent to the geometric phase for pure states. Thus, the Uhlmann phase seems to be a reasonable extension of the pure state geometric phase described in chapter 1. It is also possible to get the phase for a smooth curve of density operators by using a similar approximation method as in section 1.3.

As mentioned above, there are some complications with the Uhlmann phase. Firstly, there is no natural way to setup an experiment to measure the phase in the non-pure case, which makes it, at least presently, unsatisfying from an operational perspective. Secondly, it depends not only on the geometry of the path of density operators but also on the evolution in the extended Hilbert space itself [13]. These issues motivate the search for further approaches to mixed state geometric phases.

2.2 Sjöqvist *et al.*'s phase

In [12] Sjöqvist *et al.* provide "a new formalism of the geometric phase for mixed states in the experimental context of quantum interferometry". Given that the

traditional way to observe pure state phases is interferometry, such methods could also be considered a natural way to extend the geometric phase to mixed states.

If we use a standard interferometer of Mach-Zehnder type, as in figure 2.1, it is possible to extend the spatial (pure) input state $\rho = |0\rangle\langle 0|$ with an additional internal degree of freedom ρ_{in} so that the total input becomes a composite of a pure and a mixed state:

$$\rho_{total} = \rho_0 \otimes \rho_{in}. \quad (2.13)$$

After the first beam splitter we introduce a unitary transformation U which oper-

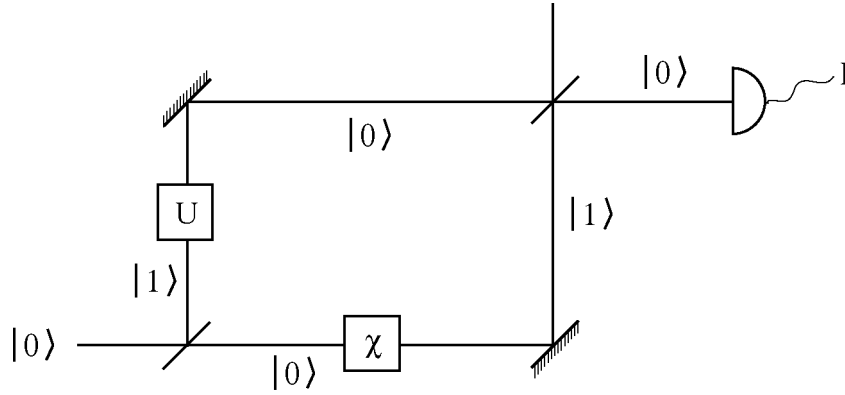


Figure 2.1: Mach-Zehnder interferometer

ates on ρ_{in} along the $|1\rangle$ -path. As in the pure state case, there is also a phase shift χ which operates on ρ_{in} along the $|0\rangle$ -path. All other operations, such as beam splitters and mirrors, are assumed to not influence ρ_{in} . The output intensity along $|0\rangle$ in this interferometry setup is [12]

$$I \propto 1 + |\text{Tr}(U\rho_0)| \cos(\chi - \arg \text{Tr}(U\rho_0)). \quad (2.14)$$

As expected, there will be oscillations in the intensity by the variable χ phase shift; but there will also be an additional shift. This shift, equal to $\arg \text{Tr}(U\rho_0)$, depends only on the mixed part of the input state, and its evolution U , so it is tempting to take this as our mixed state phase Φ . We choose to do so and investigate its behavior for a pure state $\rho_0 = |\psi_0\rangle\langle\psi_0|$:

$$\Phi = \arg \text{Tr}(U\rho_0) = \arg \text{Tr}(U|\psi_0\rangle\langle\psi_0|) = \arg \langle\psi_0|U|\psi_0\rangle. \quad (2.15)$$

It turns out to be equal to the ordinary Pancharatnam phase between $|\psi_0\rangle$ and $U|\psi_0\rangle$. Thus we conclude that this phase is a valid mixed state extension of the Pancharatnam phase.

We have found a way to express the total relative phase for mixed state evolutions. But what about geometric phases? It is clear that Φ as given in (2.15) cannot be used to construct invariant expressions in the same way as for pure states, since Φ does not depend explicitly on the two separate states. Instead, another idea derived from the theory of pure state phases can be used: parallel transportation.

In section 1.2 we saw how the geometric phase could be interpreted as a holonomy effect from parallel transportation. The idea in [12] is to get the geometric phase by establishing parallel transport of ρ_0 in the space of density operators. Parallel transport can be achieved by demanding that the evolution by U at any time t makes the density operator at time, called $\rho(t)$, in phase with $\rho(t + dt)$. Using the concept of phase as in (2.15), the formulation of this parallel transport condition becomes

$$\text{Tr}(\rho(0)U^\dagger(t)\dot{U}(t)) = 0. \quad (2.16)$$

This condition is analogous to the pure state parallel transport condition [15],

$$\langle \psi(0) | U^\dagger(t) \dot{U}(t) | \psi(0) \rangle = 0, \quad (2.17)$$

which can be checked by inserting a pure state density matrix in (2.16). When working with mixed states, however, the condition (2.16) is not sufficient for getting a unique parallel transport condition. It is also necessary that each individual state $|i(0)\rangle$ in $\rho(0)$ is parallel transported according to (2.17) so that

$$\langle i(0) | U^\dagger(t) \dot{U}(t) | i(0) \rangle = 0, \quad i = 1, \dots, N. \quad (2.18)$$

With these conditions on U fulfilled, the dynamical part of the phase vanishes and the geometric phase for a mixed state can be defined as

$$\phi_g = \arg \text{Tr}(U(t)\rho_0) = \arg \left(\sum_j w_j v_j e^{i\beta_j} \right), \quad (2.19)$$

which is the ensemble average of the individual pure state geometric phase factors $e^{i\beta_j}$, weighted by visibility v_j and probability w_j .

As an example of this mixed state geometric phase, we can look at a spin $\frac{1}{2}$ -particle. Its density operator can be written in terms of a Bloch vector \mathbf{r} according to

$$\rho = \frac{1}{2}(1 + \mathbf{r} \cdot \boldsymbol{\sigma}). \quad (2.20)$$

If ρ during the evolution traces out a curve on the Bloch sphere that subtends a solid angle Ω (like in figure 1.2) the geometric phase as given by (2.17) is

$$\phi_g = -\arctan \left(|\mathbf{r}| \tan \frac{\Omega}{2} \right) = -\arctan \left(r \tan \frac{\Omega}{2} \right). \quad (2.21)$$

This important example of a geometric phase for a mixed state will be used later on, when we look at mixed state phases in the context of polarimetry.

2.3 Comparison of mixed state geometric phases

We have found two ways of generalizing pure state phases. But are there any relations between Uhlmann's phase and the phase proposed by Sjöqvist *et al.*? It is not straightforward to compare (2.4) and (2.17), since they are expressed in different mathematical frameworks. In the trivial case of pure states, the phases of Uhlmann and Sjöqvist *et al.* naturally coincide [13], but for mixed states they are generally different. There are different opinions on the extent of inequivalence, however. In [13] the two approaches are shown to be equal *only* for $r = 1$ (pure states), while equivalence for $r = 1$ and $r = \sqrt{\frac{2}{3}}$ is claimed for some unitary evolutions in [16].

Chapter 3

Experimental phase measurements

Experimental verification is crucial for all theoretical predictions in physics. It was not long after Berry's paper in 1984 that the first direct experimental observations of geometric phases were made [17, 18, 19]. Tomita and Chiao [17] sent linearly polarized light through a coiled optical fiber arranged so that the light entered and exited the coil in the same direction. When exiting the fiber, the light had acquired a rotation of polarization equal to the solid angle Ω , corresponding to the area enclosed by the curve of the polarization vector on the Poincaré sphere. Thus, it is not even necessary to use quantum mechanics to understand the outcome of this experiment. It can be understood from classical optics in the same way as Pancharatnam's original set-up.

Bitter and Dubbers [18] measured the geometric phase for spin-polarized neutrons in a similar way. They sent a beam of neutrons through a static magnetic field arranged so that it slowly rotated the spin. After a full revolution, they observed a remaining rotation of the spin. This effect was of quantum mechanical origin, since the spin is a purely quantum mechanical property. The same result was also found when Richardson *et. al.* [19] used an opposite approach and took ultracold neutrons, fixed in a bottle, and subjected them to a rotating magnetic field. In both cases it was possible to extract a small geometric phase equal to $\Omega/2$.

All the early experiments used two-level systems and measured the geometric phase by polarization measurements. Phases of two-level systems are often called *SU(2) phases*, although the phases themselves are technically U(1) phases. In this context, SU(2) refers to the algebra describing the evolution of the whole system. SU(2) phases are the most commonly studied, partly because there have been more theoretical work on them, and partly due to the lack of versatile experimental systems with spin $> \frac{1}{2}$. But there are other ways than polarimetry to observe phases, as will be outlined later in this chapter. To elucidate more properties of quantum systems, neutron and laser interferometers have become important tools.

3.1 Strategies for observing phases

Due to the lack of a relative phase operator, there is no other way of measuring phases known today than using some kind of interference, often by photons or neutrons. There are two different ways of accomplishing this: either by using, what I will call, "mathematically" separated states or "physically" separated states. Mathematical separation occurs in polarimetry and physical separation in interferometry.

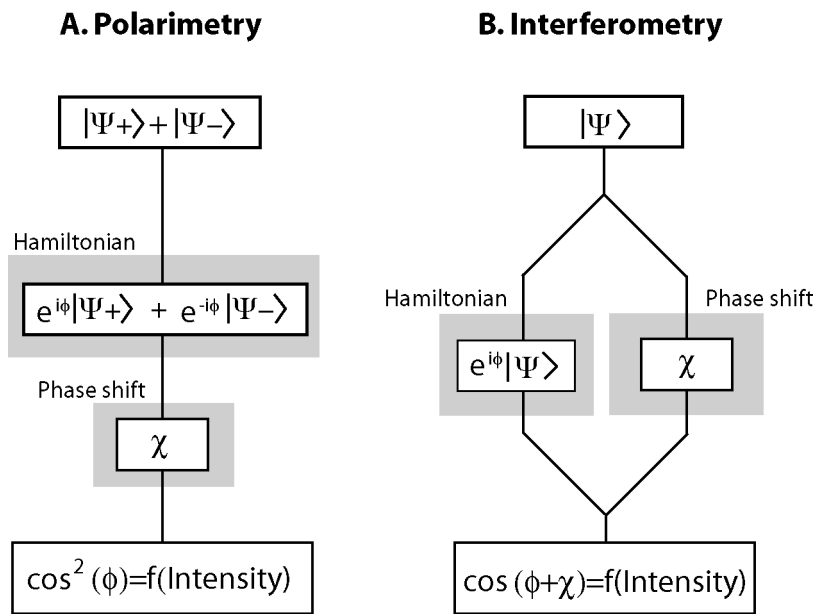


Figure 3.1: Polarimetric (A) and interferometric (B) ways of measuring SU(2) phases. In (A), the components of the superposition produce interference when measuring the intensity. In (B), two physically separated states are recombined to produce interference.

In polarimetric tests of SU(2) phases, a superposition of two orthogonal states are created by rotating $\pi/2$ around an axis perpendicular to the quantization axis of the initial state. The components of the superposition evolve under the same SU(2) Hamiltonian and acquire opposite phases. When the superposition is flipped back by a $-\pi/2$ rotation there will be "interference" between the components upon measurement along the initial quantization axis. If the evolution was cyclic, the final state differs from the initial by a rotation of ϕ about the initial axis. Otherwise, a phase shift must be inserted and the phase can then be inferred from oscillations of the intensity as measured along the initial axis.

In interferometry, waves of either neutrons or photons are coherently split and then spatially separated, followed by recombination to a single wave again. The internal state of one of the split beams undergoes a nontrivial evolution, while the

other beam is subjected to a simple phase shift. The phase shows up as the shift of the interference pattern that occurs when the phase shift is removed from the interferometer.

There are many ways of constructing experimental setups based on either the polarimetric or the interferometric approach. In the next sections we will look at two setups that enables one to measure the Pancharatnam phase for unitary, but noncyclic SU(2) evolutions. We have already seen how the interferometric way was generalized to mixed states in section 2.2, and in the next chapters we will look at further generalizations of the polarimetric way of measuring phases.

3.2 Polarimetric setup

This method [20] uses neutrons subjected to magnetic fields as a probe for SU(2) phases. Neutrons have a finite magnetic moment, but are still electrically neutral, which make them well suited for such experiments. Note, however, that the treatment is valid for all kinds of SU(2) systems, not just neutrons.

Consider an experimental arrangement as in fig. 3.2. A single beam of spin-polarized neutrons is sent through a series of devices. First a flipper, then a general SU(2) evolution, followed by another flipper, and finally the spin analyzer. A guiding magnetic field is also put over the entire setup. The key principle, which allows observations of noncyclic phases, is the translation of the flippers. They are translated so that the sum $L_0 = L + L'$ is kept constant. This produces a variation of the dynamical phase, which transforms into an oscillation of the measured intensity when the flippers are moved. The minimum and the maximum of this oscillation can be associated with the Pancharatnam phase Φ according to

$$\Phi \bmod \pi = \arccos \sqrt{\frac{I_{min}}{1 - I_{max} + I_{min}}}. \quad (3.1)$$

Let us now work this through in detail. Neutrons, which have been spin-polarized in the \mathbf{z} -direction, enter the experimental arrangement, represented by the spin state $|z\rangle$. The first spin flipper corresponds to the operator $\exp(-i\frac{\pi}{4}\sigma_y)$. Before reaching the zone of the SU(2) evolution, the neutrons precess an angle $\phi = -2\mu BL/\gamma$ about the \mathbf{z} -axis (γ is the neutron speed) by applying a uniform magnetic field $\mathbf{B} = B\hat{\mathbf{z}}$. The operator for this is $\exp(-i\frac{\phi}{2}\sigma_z)$. By denoting the general SU(2) evolution as U we have so far

$$|z\rangle \rightarrow U e^{-\frac{\phi}{2}i\sigma_z} e^{-\frac{\pi}{4}i\sigma_y} |z\rangle. \quad (3.2)$$

The next step is another precession. This time the distance is $L' = L_0 - L$. By choosing L_0 as $n\pi\gamma/|\mu|B$, the precession angle becomes $2n\pi - \phi$. A second

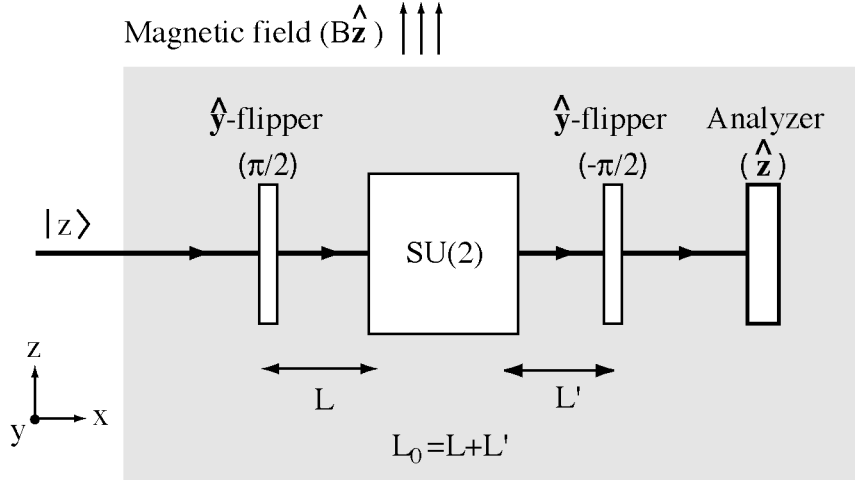


Figure 3.2: Conceptual view of the experimental set-up for measuring non-cyclic phases with polarimetry.

spin flipper completes the evolution, and operates as $\exp(\frac{\pi}{4}i\sigma_y)$. The polarization analyzer filters neutrons having spins along \hat{z} . Thus the fractional intensity it detects is:

$$\begin{aligned}
 I &= |\langle z | e^{\frac{\pi}{4}i\sigma_y} e^{-\frac{2n\pi-\phi}{2}i\sigma_z} U e^{-\frac{\phi}{2}i\sigma_z} e^{-\frac{\pi}{4}i\sigma_y} | z \rangle|^2 \\
 &= |(-1)^n \langle z | e^{\frac{\pi}{4}i\sigma_y} e^{\frac{\phi}{2}i\sigma_z} U e^{-\frac{\phi}{2}i\sigma_z} e^{-\frac{\pi}{4}i\sigma_y} | z \rangle|^2 \\
 &= |\langle z' | U | z' \rangle|^2
 \end{aligned} \tag{3.3}$$

With U represented by

$$U = \begin{pmatrix} e^{i\delta} \cos \xi & -e^{-i\zeta} \sin \xi \\ e^{i\zeta} \sin \xi & e^{-i\delta} \cos \xi \end{pmatrix}, \tag{3.4}$$

the explicit expression for the intensity becomes

$$I = \cos^2 \xi \cos^2 \delta + \sin^2 \xi \sin^2(\zeta - \phi), \tag{3.5}$$

with the extreme values:

$$\begin{aligned}
 I_{min} &= \cos^2 \xi \cos^2 \delta \\
 I_{max} &= \cos^2 \xi \cos^2 \delta + \sin^2 \xi,
 \end{aligned} \tag{3.6}$$

upon translation of the flippers. Our goal is now to extract the Pancharatnam phase from these equations. From (3.4) we see that our phase of interest is δ . Thus we form

$$\frac{I_{min}}{1 - I_{max} + I_{min}} = \cos^2 \delta \equiv \cos^2 \Phi, \tag{3.7}$$

which is equivalent to expression (3.1).

An experimental based on this approach was carried out in 1999 at a research reactor in Vienna [23]. The experiment agreed with the theoretical prediction within 1%. It was also possible to separate the geometric and the dynamical components of the measured phase by arranging so that the two phase components arose from distinct physical operators. The dynamical phase was given by the spin flipper translation, while the geometric phase was created by a parallel transport operation in the SU(2) part.

3.3 Interferometric setup

The correct way of measuring the Pancharatnam phase with an interferometer was delineated in [21]. Just as in the previous section, spin-polarized neutrons could be used as spin- $\frac{1}{2}$ particles.

Consider a Mach-Zehnder interferometer of the kind pictured in figure 3.3. A beam of particles in the $|\psi\rangle$ -state enters an interferometer and get splitted into two subbeams **1** and **2**. Each subbeam is subjected to either an U(1) phase shift or a full SU(2) evolution and the beam pair is subsequently brought to interfere. The intensity, as read from the detector along one of the beam directions (**2**), oscillates as a result of interference when the phase shift χ is varied.

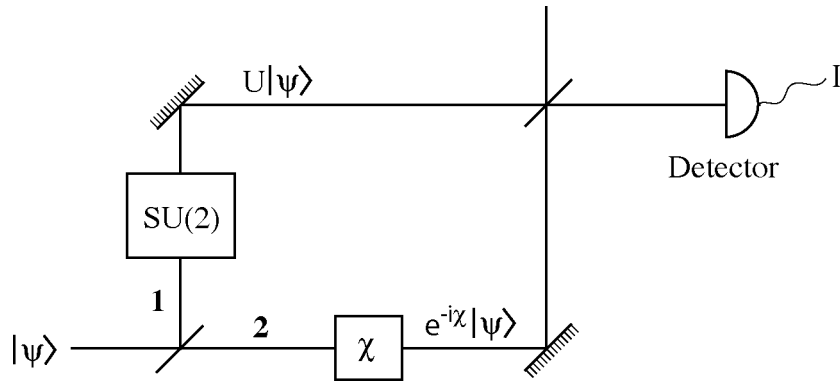


Figure 3.3: Conceptual view of the experimental setup for measuring noncyclic phases in interferometry.

We have seen earlier (2.12) that when the SU(2) operation does not affect the beam states or is absent, the intensity fluctuates as:

$$I(\chi) \propto 1 + \cos \chi. \quad (3.8)$$

If the SU(2) operation is added, however, the intensity oscillation pattern gets

modified according to

$$I(\chi, \Phi) \propto \frac{1}{2} \left(1 + \langle \psi_0 | U^\dagger U | \psi_0 \rangle \right) + \mathcal{A} \cos(\chi + \Phi). \quad (3.9)$$

This forms the basis for the interferometric observation of the Pancharatnam phase, because Φ can now be deduced from the shift of the pattern that occurs when the SU(2) operation is removed from the interferometer to yield (3.8).

An experiment according to this method was carried out at the University of Missouri [22]. It represented the first experimental separation of dynamical and geometrical phases, as well as the first direct verification of the Pauli anti-commutation relations. The SU(2) evolution yielding the geometric phase was implemented as a rotation of two identical spin flippers. The dynamical phase shift was produced by a linear translation of the two flippers (as in the polarimetric case). Confirming the theoretical predictions, the observed phase shift for the Pauli anti-commutation equaled 180° with a precision of 2%.

3.4 Polarimetry vs. Interferometry

What is the difference between observing phases polarimetrically vs. interferometrically? One difference is precision. The polarimetrically measured phases are within 1% of theory, twice the precision of the interferometric experiment. This improvement comes from a much better utilization of the neutron source in the polarimetric setup [24]. When using an interferometer, the incident neutron beam can only have an angular spread of a few arc seconds, which reduces the neutron intensity available for the experiment by several orders of magnitude. In a polarimetric set-up, however, there are no such constraints and a large fraction of the incident neutrons can be used. The higher effective intensity can then be used either to improve the precision or to perform the experiment at a low-flux reactor. Overall, the polarimetric way is a more robust method, less sensitive to spatial, mechanical, and thermal disturbances than interferometry.

Another difference is what periodicity of the phase that can be measured. The practical advantage of polarimetry may be limited by the modulo 180° property of the phase measurement. Interferometric experiments, on the other hand, measure modulo 360° , which allows verification of the Pauli anticommutation (as in [22]). The reason behind the modulo 180° property in polarimetry is that the phase is inferred from the intensity (3.5), which depends on $\cos^2 \Phi$, not $\cos \Phi$ as is the case in interferometry (3.9). Physically, this difference comes from the final $|z\rangle$ -projection in polarimetry: states with opposite phases will give the same $|z\rangle$ -intensity.

Chapter 4

Measuring higher-spin phases

In [20] Wagh and Rakhecha described how to measure the Pancharatnam phase in SU(2) polarimetry, i.e. for spin- $\frac{1}{2}$ systems, but is it possible to extend this polarimetric way of measuring the Pancharatnam phase to other systems as well? In this chapter we demonstrate polarimetry on pure states with arbitrary spin. In particular, we look at spin-coherent states that represent minimum uncertainty states. Besides pure theoretical curiosity, there are other reasons why this is of interest. We learned in the previous chapter that polarimetric experiments are easier to perform and potentially more precise. This could be of interest, since no experimental observations of higher-spin phases have been done so far. Similarly, the atomic coherent states have important applications in quantum optics [25], which is used for experimental investigations of many quantum mechanical phenomena.

4.1 SO(3) polarimetry on higher spin states

There is no simple way to extend the SU(2) method to higher SU(N) evolutions because an SU(>2) operator does not work solely as an rotation operator. This destroys the rotational symmetry of the experimental setup and leads to very complicated expressions for the output intensity.

Instead, let us look at the SU(2) method in view of spin rotations. From mathematics it is known that the SU(2) group is locally isomorphic to the group SO(3) of rotations in three-dimensional space. If we reformulate the SU(2) method in terms of SO(3) operations it should be readily extendable to higher spins. In section 3.2 we saw how the total evolution of the input state could be seen as a series of SU(2) operations. If we rewrite them as SO(3) operations we get a total operator of the form (cf. eq. 3.3)

$$U(\alpha, \beta, \gamma, \phi) = e^{i\frac{\pi}{2}J_y} e^{i\phi J_z} \tilde{U}(\alpha, \beta, \gamma) e^{-i\phi J_z} e^{-i\frac{\pi}{2}J_y} \quad (4.1)$$

with \tilde{U} replacing the general SU(2) operation.

Our first concern is to express the Pancharatnam phase in this type of evolution. If we consider an abstract $|jm\rangle$ state evolving under \tilde{U} , then

$$\begin{aligned}\Phi &= \arg\langle jm|\tilde{U}(\alpha, \beta, \gamma)|jm\rangle = \arg D_{m,m}^{(j)}(\alpha, \beta, \gamma) \\ &= \arg e^{-i(\alpha m + \gamma m)} d_{m,m}^{(j)}(\beta) = -m(\alpha + \gamma) + \arg d_{m,m}^{(j)}(\beta) \\ &\equiv m \cdot 2\delta + \Delta,\end{aligned}\tag{4.2}$$

where the last identification makes our δ equivalent to the one used by Wagh and Rakhecha [20]. The parameter Δ is related to the sign of the d -matrix element. It is always 0 or π , since the d -matrix is real. In order to find the Pancharatnam phase, one would expect the need to know Δ . In the spin- $\frac{1}{2}$ case considered earlier, however, Δ was happily ignored, because

$$\cos^2 \Phi = \cos^2(m \cdot 2\delta + \Delta) = \cos^2(\delta + 0 \vee \pi) = \cos^2 \delta.\tag{4.3}$$

This applies to other m as well:

$$\cos^2 \Phi = \cos^2(2m\delta).\tag{4.4}$$

Our second concern is to find the resulting output intensity. If the $|jm\rangle$ state is subjected to the operator U in (4.1) and the output analyzed in the same $|jm\rangle$ basis, the intensity becomes

$$I = |\langle jm|U(\alpha, \beta, \gamma, \delta)|jm\rangle|^2.\tag{4.5}$$

Now introduce a decomposition of the $|jm\rangle$ state into a direct product of spin-1/2 states u_+ and u_- (see e.g. [26]):

$$|jm\rangle = \frac{C_{jm}}{(2j)!} \sum_P u_+^{(1)} \otimes \dots \otimes u_+^{(j+m)} \otimes u_-^{(j+m+1)} \otimes \dots \otimes u_-^{(2j)}.\tag{4.6}$$

C_{jm} is a normalization constant and the summation sign over P refers to a sum of all permutations of the labels of the u states. The cases of $m = \pm j$, as in coherent states, are simplest to handle, so we will consider them separately.

4.2 The $|j \pm j\rangle$ case

In the special case of $m = \pm j$ the permutation leaves the terms unchanged and the state consists of a single term:

$$|j \pm j\rangle = u_{\pm}^{(1)} \otimes \dots \otimes u_{\pm}^{(2j)}.\tag{4.7}$$

This allows a direct decomposition of (4.3) into spin- $\frac{1}{2}$ subspace intensities when treating the operator U as a product of $U^{(i)}$ operators, each rotating the spin- $\frac{1}{2}$ subspace i separately (again see [26]):

$$U = U^{(1)} \otimes \dots \otimes U^{(2j)}. \quad (4.8)$$

Substituting (4.7) and (4.8) into (4.5) now gives

$$\begin{aligned} I &= |\langle j \pm j | U | j \pm j \rangle|^2 = \left| \langle j \pm j | \prod_{i=1}^{2j} U^{(i)} \otimes \mathbf{1} | j \pm j \rangle \right|^2 \\ &= \left| \prod_{i=1}^{2j} \langle u_{\pm} | U^{(i)} | u_{\pm} \rangle \right|^2 = \left| \langle u_{\pm} | U^{(i)} | u_{\pm} \rangle^{2j} \right|^2 \\ &= \left[I^{(j=1/2)} \right]^{2j}. \end{aligned} \quad (4.9)$$

Thus, the intensity for the $|j \pm j\rangle$ state is nothing but the product of $2j$ spin- $\frac{1}{2}$ -intensities. From (3.5), we know that the explicit spin- $\frac{1}{2}$ intensity is

$$I^{(j=1/2)} = \cos^2 \xi \cos^2 \delta + \sin^2 \xi \sin^2(\zeta - \phi). \quad (4.10)$$

Thus, for arbitrary j :

$$I^{(j)} = \left[\cos^2 \xi \cos^2 \delta + \sin^2 \xi \sin^2(\zeta - \phi) \right]^{2j}. \quad (4.11)$$

This intensity oscillates between two extreme values when the spin flippers are translated to give a variation of ϕ :

$$I_{min}^{(j)} = \left[\cos^2 \xi \cos^2 \delta \right]^{2j}, \quad (4.12)$$

$$I_{max}^{(j)} = \left[\cos^2 \xi \cos^2 \delta + \sin^2 \xi \right]^{2j}. \quad (4.13)$$

We find $\cos^2 \delta$ from:

$$\cos^2 \delta = \frac{\sqrt[2j]{I_{min}^{(j)}}}{1 - \sqrt[2j]{I_{max}^{(j)}} + \sqrt[2j]{I_{min}^{(j)}}}. \quad (4.14)$$

To use this result in the expression for the Pancharatnam phase as given in (4.4), we need to relate $\cos^2(2j\delta)$ to $\cos^2 \delta$. We proceed by expanding (4.4) in terms of Chebyshev polynomials of the first kind:

$$\cos^2 \Phi = \cos^2(2j\delta) = [\cos(2j\delta)]^2 = [T_{2j}(\cos \delta)]^2. \quad (4.15)$$

The first few cases give

$$\begin{aligned}
\cos^2 \Phi^{(1)} &= -1 + 2 \cos^2 \delta, \\
\cos^2 \Phi^{(\frac{3}{2})} &= -3 \cos \delta + 4 \cos^3 \delta, \\
\cos^2 \Phi^{(2)} &= 1 - 8 \cos^2 \delta + 8 \cos^4 \delta, \\
\cos^2 \Phi^{(\frac{5}{2})} &= 5 \cos \delta - 20 \cos^3 \delta + 16 \cos^5 \delta.
\end{aligned} \tag{4.16}$$

For even $2j$, it is a matter of simple substitution to yield the phase. Finding Φ for odd $2j$ requires some additional deduction, since we can only extract the even power $\cos^2 \delta$ from expressions like (4.11). This leaves an ambiguity of the sign of $\cos \delta$ when taking $\sqrt{\cos^2 \delta}$. But by noting that the left hand side of (4.16) is always semipositive, and by collecting the $\cos \delta$ terms of the odd expansion we get

$$0 \leq \cos \delta \cdot \tilde{T}_{(2j)}(\cos^2 \delta), \tag{4.17}$$

where $\tilde{T}_{(2j)}$ is the Chebyshev polynomial $T_{(2j:\text{odd})}$ divided by $\cos \delta$. We can infer the sign of $\cos \delta$ from this relation, since $\tilde{T}_{(2j)}$ depends only on $\cos^2 \delta$. First, we calculate $\tilde{T}_{(2j)}$ using the data from (4.14) and evaluate the sign of the result. Then we apply the inequality (4.17) to determine the sign of $\cos \delta$.

4.3 The general $|jm\rangle$ case

For general $|jm\rangle$ states, symmetrization brings a total of $(2j)!$ terms in the sum (4.6). It is not necessary to work with a fully symmetrized state, however, since the symmetrization deals only with the labelling of the u_{\pm} states, while the number of u_{+} and u_{-} states remain the same. The transformation properties are thus unaffected by the symmetrization. We only need to consider simplified states of the form:

$$|jm\rangle = C_{jm} \bigotimes_{i=1}^{j+m} u_{+} \bigotimes_{k=1}^{j-m} u_{-} \equiv C_{jm} u_{+}^{j+m} u_{-}^{j-m}. \tag{4.18}$$

From the spin-1/2 case we already know how $U^{(i)}$ acts upon u_{+} and u_{-} states:

$$\begin{aligned}
U^{(i)} u_{+}^{(i)} &= c_1 u_{+}^{(i)} + c_2 u_{-}^{(i)}, \\
U^{(i)} u_{-}^{(i)} &= c_3 u_{+}^{(i)} + c_4 u_{-}^{(i)},
\end{aligned}$$

where

$$\begin{aligned}
c_1 &= \cos \xi \cos \delta - i \sin \xi \sin(\zeta - \phi), \\
c_2 &= i \cos \xi \sin \delta + \sin \xi \cos(\zeta - \phi), \\
c_3 &= i \cos \xi \sin \delta - \sin \xi \cos(\zeta - \phi), \\
c_4 &= \cos \xi \cos \delta + i \sin \xi \sin(\zeta - \phi).
\end{aligned} \tag{4.19}$$

Thus, U applied on the state (4.17) gives (with the state labels dropped)

$$U|jm\rangle = C_{jm}(c_1u_+ + c_2u_-)^{j+m}(c_3u_+ + c_4u_-)^{j-m}. \quad (4.20)$$

We expand the product by way of the binomial theorem:

$$\begin{aligned} U|jm\rangle &= C_{jm} \sum_{\nu\mu} \binom{j+m}{\nu} \binom{j-m}{\mu} (c_1)^\nu (c_2)^{j+m-\nu} \\ &\times (c_3)^\mu (c_4)^{j-m-\mu} (u_+)^{\nu+\mu} (u_-)^{2j-\nu-\mu}, \end{aligned} \quad (4.21)$$

and identify the sum indices as $\nu + \mu \equiv j + m'$. Then,

$$(u_+)^{\nu+\mu} (u_-)^{2j-\nu-\mu} \equiv (u_+)^{j+m'} (u_-)^{j-m'} = \frac{1}{C_{jm'}} |jm'\rangle, \quad (4.22)$$

and (4.20) turns into

$$\begin{aligned} U|jm\rangle &= \sum_{m'} |jm'\rangle \frac{C_{jm}}{C_{jm'}} \sum_{\nu} \binom{j+m}{\nu} \binom{j-m}{j+m'-\nu} \\ &\times (c_1)^\nu (c_2)^{j+m-\nu} (c_3)^{j+m'-\nu} (c_4)^{\nu-m-m'} \\ &= \sum_{m'} |jm'\rangle U_{m',m}^{(j)}. \end{aligned} \quad (4.23)$$

Thus, the intensity I for an incident $|jm\rangle$ state analyzed in the $|jm'\rangle$ channel reads

$$\begin{aligned} I_{m',m}^{(j)} &= |U_{m',m}^{(j)}(\delta, \zeta, \xi, \phi)|^2 \\ &= \frac{(j+m')!(j-m)!}{(j+m)!(j-m)!} \left| \sum_{\nu} \binom{j+m}{\nu} \binom{j-m}{j+m'-\nu} \right. \\ &\times (\cos \xi \cos \delta - i \sin \xi \sin(\zeta - \phi))^\nu \\ &\times (i \cos \xi \sin \delta + \sin \xi \cos(\zeta - \phi))^{j+m-\nu} \\ &\times (i \cos \xi \sin \delta - \sin \xi \cos(\zeta - \phi))^{j+m'-\nu} \\ &\left. \times (\cos \xi \cos \delta + i \sin \xi \sin(\zeta - \phi))^{\nu-m-m'} \right|^2. \end{aligned} \quad (4.24)$$

For $m' = m$ it reduces to

$$\begin{aligned} I_m^{(j)} &= (\cos^2 \xi \cos^2 \delta + \sin^2 \xi \sin^2(\zeta - \phi))^{-2m} \\ &\times \left\{ \sum_{\nu} \binom{j+m}{\nu} \binom{j-m}{j+m-\nu} \right. \\ &\times (\cos^2 \xi \cos^2 \delta + \sin^2 \xi \sin^2(\zeta - \phi))^\nu \\ &\left. \times (\cos^2 \xi \sin^2 \delta + \sin^2 \xi \cos^2(\zeta - \phi))^{j+m-\nu} \right\}^2. \end{aligned} \quad (4.25)$$

Some examples (with $I_{-m}^{(j)} = I_m^{(j)}$):

$$\begin{aligned}
I_{1/2}^{(1/2)} &= \cos^2 \xi \cos^2 \delta + \sin^2 \xi \sin^2(\zeta - \phi), \\
I_1^{(1)} &= \left(\cos^2 \xi \cos^2 \delta + \sin^2 \xi \sin^2(\zeta - \phi) \right)^2, \\
I_0^{(1)} &= \left(\cos^2 \xi \cos 2\delta - \sin^2 \xi \cos(2(\zeta - \phi)) \right)^2, \\
I_{1/2}^{(3/2)} &= \left[\cos^2 \xi \cos^2 \delta + \sin^2 \xi \sin^2(\zeta - \phi) \right] \\
&\quad \times \left[\sin^2 \xi \left(\sin^2(\zeta - \phi) - 2 \cos^2(\zeta - \phi) \right) \right. \\
&\quad \left. + \cos^2 \xi \left(\cos^2 \delta - 2 \sin^2 \delta \right) \right]^2, \\
I_1^{(2)} &= \left[\cos^2 \xi \cos^2 \delta + \sin^2 \xi \sin^2(\zeta - \phi) \right]^2 \\
&\quad \times \left[\sin^2 \xi \left(\sin^2(\zeta - \phi) - 3 \cos^2(\zeta - \phi) \right) \right. \\
&\quad \left. + \cos^2 \xi \left(\cos^2 \delta - 3 \sin^2 \delta \right) \right]^2.
\end{aligned} \tag{4.26}$$

We proceed as before by looking for extreme points. Formally, that means solving the equation

$$\frac{\partial I_{m',m}^{(j)}}{\partial \phi} = 0. \tag{4.27}$$

Most of the solutions depend on unknown variables such as ξ , but there are always two trivial solutions, similar to those of the spin- $\frac{1}{2}$ case. They are $\phi = \zeta$ or $\phi = \zeta \pm \frac{\pi}{2}$. Let us call the corresponding intensities I_1 and I_2 , respectively. The problem of determining $\cos^2 \delta$ can be put as solving the nonlinear equation system

$$\begin{aligned}
I_1 &= f_1(\cos^2 \delta, \cos^2 \xi), \\
I_2 &= f_2(\cos^2 \delta, \cos^2 \xi).
\end{aligned} \tag{4.28}$$

From the inverse function theorem, we expect to find solutions for the independent variables if the Jacobian determinant is non-zero:

$$\left| \begin{array}{cc} \frac{\partial f_1}{\partial \cos^2 \delta} & \frac{\partial f_1}{\partial \cos^2 \xi} \\ \frac{\partial f_2}{\partial \cos^2 \delta} & \frac{\partial f_2}{\partial \cos^2 \xi} \end{array} \right| \neq 0. \tag{4.29}$$

When $\cos^2 \delta$ has been determined as a function of I_1 and I_2 , it can be inserted into equation 4.14 to give the phase. We will abstain from working out general solutions and instead look at some cases with $m \neq j$ from (4.25).

For all $m = 0$, the phase is trivially 0 or π , since:

$$\cos^2 \Phi = \cos^2(2m\delta) = \cos^2 0. \tag{4.30}$$

We note that although the intensity and $\cos^2 \delta$ can be calculated for the $m = 0$ cases (see e.g. $I_0^{(1)}$ in eq. 4.26), they are completely unrelated to the Pancharatnam phase because δ does not appear in the phase expression.

So far, we have covered the spin- $\frac{1}{2}$ and spin-1 cases completely for all m . Moving up a step in spin would give $\frac{3}{2}$. Section 4.2 tells us how to find the phase for $j = m = \frac{3}{2}$. This leaves one case: $j = \frac{3}{2}, m = \pm\frac{1}{2}$. The intensity for this case was given in (4.26). Putting $\phi = \zeta$ and $\phi = \zeta \pm \frac{\pi}{2}$ give the two extreme values

$$\begin{aligned} I_1 &= [\cos^2 \xi \cos^2 \delta + \sin^2 \xi] [\cos^2 \xi (\cos^2 \delta - 2 \sin^2 \delta) + \sin^2 \xi], \\ I_2 &= [\cos^2 \xi \cos^2 \delta] [\cos^2 \xi (\cos^2 \delta - 2 \sin^2 \delta) - 2 \sin^2 \xi]. \end{aligned} \quad (4.31)$$

It can be shown by evaluating the Jacobian matrix that this system is not generally solvable for all values of ξ and δ . There are still singularities around $\xi = \frac{\pi}{2}$ and $\delta = \frac{\pi}{2}$, just as in the spin- $\frac{1}{2}$ case. But locally, the system is solvable. The right-hand side of the expressions in (4.31) are polynomials in $\cos^2 \delta$ and $\cos^2 \xi$ to the second degree and are easy to solve. The resulting solutions are still complicated, however, so in order to present smaller expressions we expand (4.31) to first order in $\cos^2 \xi$. This approximation is good around $\xi = \frac{\pi}{2}$, which could be used to investigate convergence of the phase at the singularity point. Solving (4.31) for $\cos^2 \delta$ now gives

$$\cos^2 \delta \approx \frac{2I_1}{-1 + 2I_1 + I_2}. \quad (4.32)$$

The phase could then be calculated from

$$\cos^2 \Phi^{(\frac{3}{2}, \frac{1}{2})} = \cos^2 \delta, \quad (4.33)$$

as described by (4.4). Extending the method to higher spins should be straightforward. The next interesting case would be $j = 2, m = 1$ (the middle case $j = 2, m = 0$ is trivial according to eq. 4.30). Using the same approximation yields

$$\begin{aligned} \cos^2 \delta &\approx \frac{5\sqrt{I_1}}{-3 + 5\sqrt{I_1} + 3\sqrt{I_2}}, \\ \cos^2 \Phi^{(2,1)} &= 2\cos^2 \delta - 1. \end{aligned} \quad (4.34)$$

But due to polynomial nature of the equation system used to acquire $\cos^2 \delta$ it is likely that, at some point, the polynomial degree will become too high to allow analytical solutions. Fortunately, there is always the option of using approximations or numerical methods.

Experimentally, though, there is a problem which we have not touch upon: how to identify the extreme points I_1 and I_2 . In the $|jj\rangle$ case, there were only two

extreme points, which can always be recognized, just by plotting the intensity as a function of ϕ . But as the spin number increases and $|m| < j$, the number of extreme points increase as well. For a $|21\rangle$ state, four extreme points are visible (fig. 4.1). Without further information, we would not be able to identify I_1 and I_2 among the four. But luckily, $\phi_1 - \phi_2 = \pm \frac{\pi}{2}$ always hold for those intensities. This allows us to find the two extreme points needed for eq. 4.28, just by comparing the distances between the different extreme points. In all but the most symmetric cases, this method is likely to be applicable.

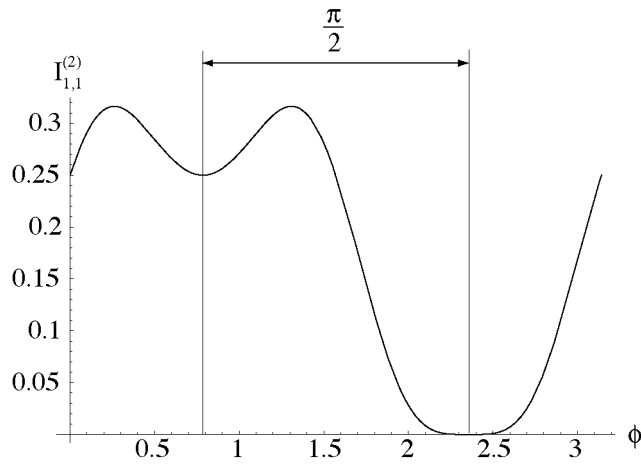


Figure 4.1: The output intensity when a $|21\rangle$ state is subjected to an evolution with the parameters $\zeta = \xi = \delta = \pi/4$. When the dynamical phase ϕ is varied, the intensity oscillates between a series of minima and maxima. The extreme points we are interested in are always separated by $\frac{\pi}{2}$.

Chapter 5

Mixed states in polarimetry

The Pancharatnam phase for mixed states was discussed by Uhlmann in the context of purifications, and by Sjöqvist *et al.* in the context of interferometry. In this chapter we will look at how to measure mixed spin-1/2 state phases by *polarimetry*. As with higher-spin phases, polarimetry offers experimental advantages. Thus, a polarimetric implementation of the mixed state phase described in interferometry [12] could make it less complicated to conduct an experiment to observe this new phase.

5.1 Evolution of the mixed state

Suppose that a mixed state entering the Wagh and Rakhecha experimental setup (see fig. 3.2) is described by the following density operator

$$\rho_{in} = \frac{1}{2} (1 + r\sigma_z). \quad (5.1)$$

If the total evolution within the arrangement is governed by the unitary operator U the output state is:

$$\rho_{out} = U\rho_{in}U^\dagger. \quad (5.2)$$

Measurement with the projection operator $|z\rangle\langle z|$ yields a fractional intensity

$$I^p = \text{Tr}(|z\rangle\langle z|\rho_{out}) \quad (5.3)$$

of neutrons with spin in the z -direction. Inserting (5.1) into (5.3) we obtain

$$I^p = \frac{1+r}{2} \text{Tr}(|z\rangle\langle z|U|z\rangle\langle z|U^\dagger) + \frac{1-r}{2} \text{Tr}(|z\rangle\langle z|U|-z\rangle\langle -z|U^\dagger) \quad (5.4)$$

using the linear property of the trace. By noticing that $\text{Tr}(|z\rangle\langle z|U|z\rangle\langle z|U^\dagger)$ and $\text{Tr}(|z\rangle\langle z|U|-z\rangle\langle -z|U^\dagger)$ are in fact the pure state output intensities of $|z\rangle$ and

$| - z \rangle$ measured in the $| z \rangle$ direction, we arrive at the following simple expression for the mixed state intensity:

$$I^\rho = \frac{1+r}{2} I_{\frac{1}{2}, \frac{1}{2}} + \frac{1-r}{2} I_{\frac{1}{2}, -\frac{1}{2}}. \quad (5.5)$$

Recalling that

$$I_{\frac{1}{2}, \frac{1}{2}} = \cos^2 \xi \cos^2 \delta + \sin^2 \xi \sin^2(\zeta - \phi), \quad (5.6)$$

$$I_{\frac{1}{2}, -\frac{1}{2}} = \cos^2 \xi \sin^2 \delta + \sin^2 \xi \cos^2(\zeta - \phi) \quad (5.7)$$

gives the explicit expression

$$I^\rho = \frac{1+r}{2} \left[\cos^2 \xi \cos^2 \delta + \sin^2 \xi \sin^2(\zeta - \phi) \right] \quad (5.8)$$

$$+ \frac{1-r}{2} \left[\cos^2 \xi \sin^2 \delta + \sin^2 \xi \cos^2(\zeta - \phi) \right],$$

which reduces to

$$I^\rho = \frac{1}{2} \left[1 + r \{ \cos^2 \xi \cos 2\delta - \sin^2 \xi \cos 2(\zeta - \phi) \} \right]. \quad (5.9)$$

5.2 Generalizing the pure state Pancharatnam phase to the mixed state

In [20] Wagh and Rakhecha extracted the Pancharatnam phase by combining the minimum and the maximum of the pure state total intensity:

$$\cos^2 \Phi = \frac{I_{min}}{1 - I_{max} + I_{min}}. \quad (5.10)$$

Can something similar be done with the mixed state intensity (5.9) giving a mixed state phase? The maximum and minimum of (5.9) upon translation of the flippers are

$$I_{min}^\rho = \frac{1}{2} \left(1 + r \cos^2 \xi \cos 2\delta + r \sin^2 \xi \right), \quad (5.11)$$

$$I_{max}^\rho = \frac{1}{2} \left(1 + r \cos^2 \xi \cos 2\delta - r \sin^2 \xi \right) \quad (5.12)$$

for $r > 0$. Unfortunately, direct insertion of these new extrema into (5.10) gives an unsatisfactory result because this phase fails to satisfy one basic requirement for a well-behaved generalization, namely: $\Phi \rightarrow 0$ as $r \rightarrow 0$. Instead we can

try to construct generalized expressions that fulfill this requirement. Starting from (5.10) we attach variable coefficients $c_i(r)$ to each term:

$$\cos^2 \Phi = \frac{c_1(r)I_{min}}{c_2(r) - c_3(r)I_{max} + c_4(r)I_{min}}. \quad (5.13)$$

(Note that for (5.13) and all following equations, I refers to mixed state intensities.) It is possible to fulfill the zero phase condition and still yield (5.10) for $r = 1$ by choosing the coefficients so that $c_i(1) = 1$ and $c_1(0) = 0$. There are, however, an infinite number of such generalized expressions to choose from. Say that we add an additional, completely general, function $g(r, I_{min}, I_{max})$ to the expression. Just by ensuring that it disappears when $r \rightarrow 1$ we have a new valid expression

$$\cos^2 \Phi = \frac{c_1(r)I_{min} + \frac{1-r}{2}g(r, I_{min}, I_{max})}{c_2(r) - c_3(r)I_{max} + c_4(r)I_{min} + \frac{1-r}{2}g(r, I_{min}, I_{max})}. \quad (5.14)$$

This can be seen as a manifestation of the fact that there exists an infinite number of curves that pass through two given points. Some additional examples of phase expressions generated by this procedure are:

$$\cos^2 \Phi = \frac{I_{min} + \frac{1-r}{2}g(r, I_{min}, I_{max})}{r^n(\frac{1+r}{2} - I_{max}) + I_{min} + \frac{1-r}{2}g(r, I_{min}, I_{max})}, \quad (5.15)$$

$$\cos^2 \Phi = \frac{(1 - r^n)(\frac{1+r}{2} - I_{max}) + I_{min} + \frac{1-r}{2}g(r, I_{min}, I_{max})}{\frac{1+r}{2} - I_{max} + I_{min} + \frac{1-r}{2}g(r, I_{min}, I_{max})}. \quad (5.16)$$

To narrow the number of cases further constraints are necessary. One such constraint is that the mixed state phase in the context of polarimetry should be the same as the one found by Sjöqvist *et al.* [12] in the context of interferometry.

5.3 Reverse engineering the mixed state phase found in interferometry

In the framework used here, the interferometric phase reads:

$$\cos^2 \Phi = \frac{1}{1 + r^2 \tan^2 \delta}. \quad (5.17)$$

To construct a new phase expression yielding (5.17) we start by solving for $\cos^2 \xi$ in (5.12) and inserting the result into (5.11):

$$I_{min} = \frac{1}{2} \left(\frac{1 - I_{max} - (I_{min} - r) \cos 2\delta}{\sin^2 \delta} \right). \quad (5.18)$$

This expression is independent of ξ and all that is needed now is to express δ in terms of Φ . Solving for δ in (5.17) gives

$$\begin{aligned}\sin^2 \delta &= 1 - \frac{r^2}{\tan^2 \Phi + r^2}, \\ \cos 2\delta &= 1 - 2 \sin^2 \delta = \frac{2r^2}{\tan^2 \Phi + r^2} - 1.\end{aligned}\quad (5.19)$$

Insertion of (5.19) into (5.18) produces an equation relating Φ to I_{min} and I_{max} :

$$I_{min} = \frac{1}{2} \left(\frac{1 - I_{max} - (I_{min} - r) \left(\frac{2r^2}{\tan^2 \Phi + r^2} - 1 \right)}{1 - \frac{r^2}{\tan^2 \Phi + r^2}} \right).\quad (5.20)$$

Solving for $\tan^2 \Phi$ unveils the expression

$$\tan^2 \Phi = \frac{r^2 \left(\frac{1+r}{2} - I_{max} \right)}{I_{min} + \frac{1-r}{2}}\quad (5.21)$$

or equivalently

$$\cos^2 \Phi = \frac{I_{min} - \frac{1-r}{2}}{r^2 \left(\frac{1+r}{2} - I_{max} \right) + I_{min} - \frac{1-r}{2}}.\quad (5.22)$$

Equations (5.21) and (5.22) show how to extract the mixed state phase from polarimetric measurements using the experimental setup described in [12]. These equations are consistent with the pure state case since putting $r = 1$ reduces the equations to the Pancharatnam phase given by (5.10). Remembering the class of phase expressions given by (5.15), one sees that expression (5.22) is found by letting $n = 2$ and $g(r, I_{min}, I_{max}) = 1$.

From an observational point of view, however, there is a problem with equations (5.21) and (5.22). To calculate the phase we need to *know* the value r , that is the degree of mixing of the incident state. It is true that r also appears in the expression for the interferometric phase (5.17), but in that case the phase is measured directly, not by proxy measurement as in polarimetry. Thus, we need to devise a way to measure r as well.

5.4 Measuring the degree of mixing

Information about the degree of mixing can be found in several ways: either by doing a second, distinct measurement on the system or by a dual-beam arrangement (fig. 5.1). In the dual-beam situation (fig. 5.1A), a source producing entangled particle pairs (see e.g.[27]) is used to allow simultaneous measurements on

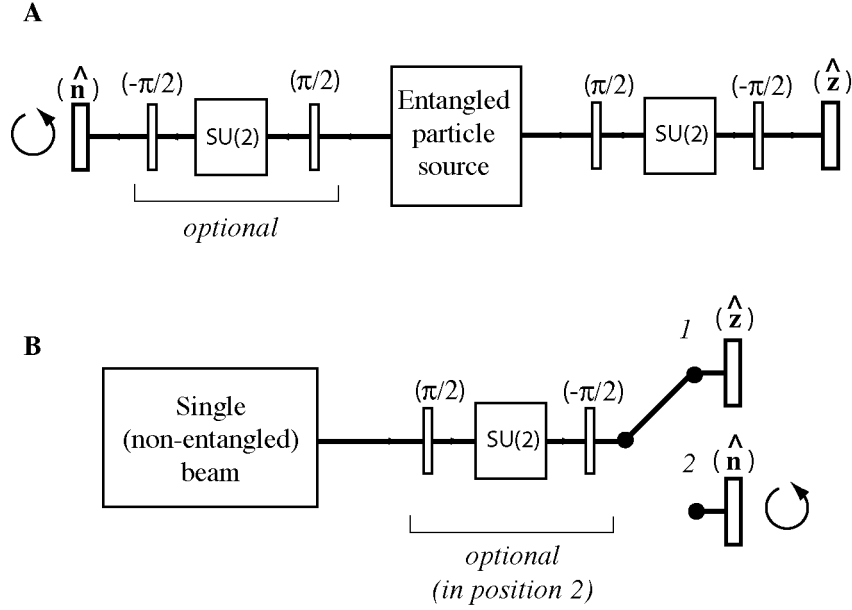


Figure 5.1: Two different ways of arranging the set-up to measure the parameter r . **A** shows an entangled dual-beam approach with simultaneous measurements. **B** shows how two repeated measurements can yield r , the first measurement (1) is in the usual z -direction, while the second (2) utilize a variation of direction.

two beams. In an actual experimental situation, the use of two repeated measurements (fig. 5.1B) is likely to be preferable, since entangled beams result in much lower intensity. Conceptually, though, dual-beam measurements offer a more pure quantum mechanical situation, in the sense that information about phase and r are obtained from measurement of the same particle pairs. Here, we look at the single-beam approach. Consider again the input state

$$\rho_{in} = \frac{1}{2}(1 + r\sigma_z) = \frac{1+r}{2}|z\rangle\langle z| + \frac{1-r}{2}| -z\rangle\langle -z|. \quad (5.23)$$

Suppose also that we keep all previous experimental equipment between the beam source and the analyzer, so that the neutrons evolve as before. We then analyze the fractional neutron intensity in an *arbitrary* direction \mathbf{n} . The intensity will become:

$$\tilde{I} = \frac{1}{2} + \frac{r}{2}(|\langle \mathbf{n}|U|z\rangle|^2 - |\langle \mathbf{n}|U|-z\rangle|^2). \quad (5.24)$$

Here U denote the total evolution operator (as in chapter 4). If the direction \mathbf{n} is varied (e.g. by rotating the spin analyzer), the intensity will again oscillate between two extrema:

$$\tilde{I}_{min} = \frac{1-r}{2},$$

$$\tilde{I}_{max} = \frac{1+r}{2}. \quad (5.25)$$

We can then easily extract r by forming

$$r = \Delta\tilde{I} = \tilde{I}_{max} - \tilde{I}_{min}. \quad (5.26)$$

(The dual-beam approach can be derived analogously, using purifications, and yields the same result.) With this knowledge, the phase expressions in section 5.3 can now be given in an operationally well defined way:

$$\begin{aligned} \tan^2 \Phi &= \frac{\Delta\tilde{I}^2(\tilde{I}_{max} - I_{max})}{I_{min} + \tilde{I}_{min}}, \\ \cos^2 \Phi &= \frac{I_{min} - \tilde{I}_{min}}{\Delta\tilde{I}^2(\tilde{I}_{max} - I_{max}) + I_{min} - \tilde{I}_{min}}. \end{aligned} \quad (5.27)$$

In comparison with the interferometric way of measuring the phase, the procedure of rotating the spin analyzer, can be seen as analogous to the phase calibration of the interferometer. It is performed by removing the part responsible for the SU(2) evolution and doing another measurement. In the polarimetric case, it is not necessary to remove the SU(2) part –one still yields (5.26).

Conclusion

The research work in my thesis has been concerned with extending the polarimetric way of measuring phases [20] to new systems. In chapter 4, I demonstrated that polarimetry could indeed be performed to measure the relative phase of $|jm\rangle$ states, using the same experimental setup as in the spin- $\frac{1}{2}$ case. The calculations needed to determine the phase from the measured intensity turned out to be increasingly more complex as the spin number increases. In principle, though, the method should be applicable to most situations, using a numerical or approximate method.

The special case of $m = j$ is especially interesting, since the coherent spin states can be expressed as: $|\mathbf{n}; j\rangle = e^{-i\mathbf{n}\cdot\mathbf{J}}|j, j\rangle_z$. Getting the phase for such states was surprisingly easy. It behaves almost like the spin- $\frac{1}{2}$ case.

In chapter 5, I investigated mixed state phases in polarimetry. It was difficult to find a specific, *a priori* mixed state phase expression. However, using the mixed state phase found by Sjöqvist *et al.* as a starting point, a method for measuring this phase in polarimetry was worked out.

In my opinion, polarimetry presents a more clean approach to measuring phases. Why should one need an interferometer to measure a property that originates not from the states themselves, but rather the evolution? I think that demonstrating these additional applications of the polarimetric way of measuring phases could help to add a sense of theoretical completeness, which could indicate a dual correspondence between interferometry and polarimetry, which I would like to think is always possible.

The use of polarimetry also offers some important practical advantages. Interferometers are tricky to handle in general. Any commercial applications of phase effects, such as the use of geometric phases in quantum computing, must most likely be implemented using polarimetry. The methods that were discovered here may not be suitable for large-scale implementation either, but hopefully the theoretical possibility could stimulate further research.

this page intentionally left blank

Acknowledgement

My greatest gratitude goes to my supervisor Erik Sjöqvist for his continuous guidance, inspiration, and enthusiasm. He gave me the opportunity to jump into a new field with a chance to do real science. Not everyone would give such a chance to someone so new to physics.

I would like to thank everybody at the Department of Quantum Chemistry for help with various problems, a bunch of great courses that eventually led to this work, for nice coffee breaks and for letting me do this work as a part-time arrangement, providing me with office facilities and resources for well over a year.

I would also like to acknowledge indirect support from the Faculty of Medicine and Pharmacy and the Division of Toxicology for their summer research scholarship. Although the scholarship concerned studies of oxidative DNA damage, I was actually able to put in a lot of work on quantum mechanics as well, during long electrophoresis runs.

In addition, there are many people and things that I would like to acknowledge due to their importance in my work. Unfortunately, I think it is not practical to list all because then I would be reciting names of many that I never met, but whose works of one kind or another has inspired me. Suffice it to say that it includes all those from Apple, the computer company, to Stephen Wolfram, inventor of Mathematica.

Thank you, and be well and happy!

this page intentionally left blank

Bibliography

- [1] M.V. Berry. *Quantal phase factor accompanying adiabatic changes*, **1984**. Proc. Roy. Soc. London Ser. A 392:45-57.
- [2] Y. Aharonov, J. Anandan. *Phase change during a cyclic quantum evolution*, **1987**. Phys. Rev. Lett. 58:1593-1596.
- [3] E. Sjöqvist. *Proposed interferometry test of noncyclic geometric phase*, **2001**. Phys. Lett. A 286:4-6.
- [4] S. Pancharatnam. *Generalized theory of interference, and its applications*, **1956**. Proc. Indian Acad. Sci. A 44:247-262.
- [5] S. Ramaseshan, R. Nityananda. *The interference of polarized light as an early example of Berry's phase*, **1986**. Curr. Sci. 55:1225.
- [6] M.V. Berry. *The Adiabatic Phase and Pancharatnam Phase for Polarized Light*, **1987**. J. Mod. Opt. 34(11):1401-1407.
- [7] V. Bargmann. *Note on Wigner's theorem on symmetry operations*, **1964**. J. Math. Phys. 5:862-868.
- [8] J.H. Hannay. *Angle variable holonomy in adiabatic excursion of an integrable Hamiltonian*, **1985**. J. Phys. A. 18:221-230.
- [9] N. Mukunda, R. Simon. *Quantum kinematic approach to the geometric phase: I. General formalism*, **1993**. Ann. Phys. (N.Y.) 228:205-268.
- [10] J.A. Jones, V. Vedral, A. Ekert, G. Castagnoli. *Geometric quantum computation using nuclear magnetic resonance*, **2000**. Nature 403:869-871.
- [11] A. Uhlmann. *Parallel transport and "quantum holonomy" along density operators*, **1986**. Rep. Math. Phys. 24:229-240.
- [12] E. Sjöqvist, A.K. Pati, A. Ekert, J.S. Anandan, M. Ericsson, D.K.L. Oi, V. Vedral. *Geometric phases for mixed states in interferometry*, **2000**. Phys. Rev. Lett. 85:2845-2849.

- [13] M. Ericsson, A.K. Pati, E. Sjöqvist, J. Brännlund, D.K.L. Oi. *Mixed state geometric phases, entangled systems, and local unitary transformations*, **2002**. quant-ph/0206063
- [14] G.G. Emch. *Algebraic Methods in Statistical Mechanics and Quantum Field Theory*, **1972**. Wiley-Interscience, New York.
- [15] J. Anandan. *The Geometric Phase*, **1992**. Nature 360:307-313.
- [16] P.B. Slater. *Mixed state holonomy*, **2002**. Lett. Math. Phys. 60:123-133.
- [17] A. Tomita, R.Y. Chiao. *Observation of Berry's topological phase by use of an optical fiber*, **1986**. Phys. Rev. Lett. 57:937-940.
- [18] T. Bitter, D. Dubbers. *Manifestation of Berry's topological phase in neutron spin rotation*, **1987**. Phys. Rev. Lett. 59:251-254.
- [19] D.J. Richardson, A.J. Kilvington, K. Green, S.K. Lamoreaux. *Demonstration of Berry's Phase Using Stored Ultracold Neutrons*, **1988**. Phys. Rev. Lett. 61:2030-2033.
- [20] A.G. Wagh, V.C. Rakhecha. *On measuring the Pancharatnam phase. II. SU(2) polarimetry*, **1995**. Phys. Lett. A. 197:112-115.
- [21] A.G. Wagh, V.C. Rakhecha. *On measuring the Pancharatnam phase. I. Interferometry*, **1995**. Phys. Lett. A. 197:107-111.
- [22] A.G. Wagh, V.C. Rakhecha, J. Summhammer, G. Badurek, H. Weinfurter, B.E. Allman, H. Kaiser, K. Hamacher, D.L. Jacobson, S. A. Werner. *Experimental separation of geometric and dynamical phases using neutron interferometry*, **1997**. Phys. Rev. Lett. 78:755-759.
- [23] A.G. Wagh, G. Badurek, V.C. Rakhecha, R.J. Buchelt, A. Schriker. *Neutron polarimetric separation of geometric and dynamical phases*, **2000**. Phys. Lett. A 268:209-216.
- [24] V.C. Rakhecha, A.G. Wagh. *Observing SU(2) phases with neutrons*, **2001**. Pramana-J. Phys. 56:287-303.
- [25] W.M. Zhang, D.H. Feng, R. Gilmore. *Coherent states: Theory and some applications*, **1990**. Rev. Mod. Phys. 62:867-927.
- [26] M. Chaichian, R. Hagedorn. *Symmetries in Quantum Mechanics*, **1998**. Institute of Physics Publishing, Bristol.
- [27] A.G. White, D.F.V. James, P.H. Eberhard, P.G. Kwiat. *Nonmaximally Entangled States: Production, Characterization, and Utilization*, **1999**. Phys. Rev. Lett. 83:3103-3107.